Mannose-recognition mutant of the galactose/N-acetylgalactosamine-specific C-type lectin CEL-I engineered by site-directed mutagenesis

Hiromi Moriuchi [a], Hideaki Unno [a], Shuichiro Goda [a], Hiroaki Tateno [b], Jun Hirabayashi [b], and Tomomitsu Hatakeyama [a,*]

[a] *Laboratory of Biomolecular Chemistry, Graduate School of Engineering, Nagasaki University, 1-14 Bunkyo-machi, Nagasaki 852-8521, Japan*

[b] *Research Center for Stem Cell Engineering, National Institute of Advanced Industrial Science and Technology, Tsukuba 305-8568, Japan*

Keywords: carbohydrate; C-type lectin; site-directed mutagenesis; X-ray crystallography

---

Abbreviations: CD, circular dichroism; CRD, carbohydrate-recognition domain; CTLD, C-type lectin-like domain; EDTA, ethylenediamine tetraacetate; PAA, polyacrylamide; PD, polyamidoamine dendrimer; MBL, mannose-binding lectin; TBS, Tris-buffered saline; WT, wild-type.

The atomic coordinates and structure factors for the CEL-I/mannose complex have been deposited in the Protein Data Bank, www.pdb.org (PDB ID: 4WQQ).

* Corresponding author: Biomolecular Chemistry Laboratory, Graduate School of Engineering, Nagasaki University, 1-14 Bunkyo-machi, Nagasaki 852-8521, Japan. Tel: +81-95-819-2686; Fax: +81-95-819-2686

E-mail address: thata@nagasaki-u.ac.jp

Abstract

Background: CEL-I is a galactose/N-acetyl-galactosamine-specific C-type lectin isolated from the sea cucumber *Cucumaria echinata*. Its carbohydrate-binding site contains a QPD (Gln-Pro-Asp) motif, which is generally recognized as the galactose specificity-determining motif in the C-type lectins. In our previous study, replacement of the QPD motif by an EPN (Glu-Pro-Asn) motif led to a weak binding affinity for mannose. Therefore, we examined the effects of an additional mutation in the carbohydrate-binding site on the specificity of the lectin.

Methods: Trp105 of EPN-CEL-I was replaced by a histidine residue using site-directed mutagenesis, and the binding affinity of the resulting mutant, EPNH-CEL-I, was examined by sugar-polyamidoamine dendrimer assay, isothermal titration calorimetry, and glycoconjugate microarray analysis. Tertiary structure of the EPNH-CEL-I/mannose complex was determined by X-ray crystallographic analysis.

Results: Sugar-polyamidoamine dendrimer assay and glycoconjugate microarray analysis revealed a drastic change in the specificity of EPNH-CEL-I from galactose/N-acetyl-galactosamine to mannose. The association constant of EPNH-CEL-I for mannose was determined to be 3.17×10^3 M^{-1} at 25°C. Mannose specificity of EPNH-CEL-I was achieved by stabilization of the binding of mannose in a correct orientation, in which the EPN motif can form proper hydrogen bonds with 3- and 4-hydroxy groups of the bound mannose.

Conclusions: Specificity of CEL-I can be engineered by mutating a limited number of amino acid residues in addition to the QPD/EPN motifs.

General significance: Versatility of the C-type carbohydrate-recognition domain structure in the recognition of various carbohydrate chains could become a promising platform to develop novel molecular recognition proteins.

1. Introduction

Lectins (carbohydrate-binding proteins) are known to play important roles in molecular and cellular recognition systems in organisms. While many plant lectins have been isolated from storage tissues such as seeds and tubers, animal lectins have been found in various tissues and body fluids, reflecting their diverse structures and functions. Among the animal lectin families, C-type lectins, which were named because of their Ca^{2+} dependence, contain C-type carbohydrate-recognition

domains (CRDs)[2] usually composed of 110–130 amino acid residues, which share a common amino acid sequence homology as well as similar tertiary structures [1-3]. While the C-type CRDs often function as carbohydrate-recognition modules in cooperation with distinct domains having different biological activities [3], particularly in immune systems [4-8], invertebrate organisms also utilize C-type lectins in the innate immune system [9]. We have been investigating three Ca^{2+}-dependent lectins, CEL-I, CEL-III, and CEL-IV, from the sea cucumber *Cucumaria echinata* [10]. Among these, CEL-III is a unique ricin-type (R-type) lectin that exerts strong hemolytic and cytotoxic activities by forming membrane pores in target cells [11], whereas CEL-I and CEL-IV belong to the C-type lectins [12, 13]. These lectins may play important roles in defense against foreign organisms through their cytotoxicity or opsonization by binding to surface carbohydrates.

The carbohydrate-binding site of many C-type CRDs contains the sequence motifs QPD (Gln-Pro-Asp) and EPN (Glu-Pro-Asn), which are known to be closely related to galactose or mannose specificities. Strong evidence for this has been demonstrated by the site-directed mutagenesis study on the mannose-binding lectin MBP-A [14], in which its EPN motif was changed to a QPD motif. The resulting mutant exhibited galactose specificity, although it was relatively weak. In addition, the replacement of the residues on the basis of the structures of other galactose-binding CRDs resulted in a much increased affinity for galactose or N-acetylgalactosamine [15, 16], suggesting the importance of stabilization of the bound carbohydrates by surrounding residues in the binding site. Other reports have also shown alterations in the specificity of the C-type CRDs in surfactant proteins from mannose to galactose by changing the EPN motif to a QPD motif [17, 18]. However, to our knowledge, no report has described a specificity change from galactose to mannose in the C-type CRDs. We have previously described that the site-directed mutant EPN-CEL-I, in which the EPN motif (residues 101–103) was replaced by a QPD motif, exhibited relatively weak mannose specificity, although there was a substantial affinity for galactose [19]. This observation also suggested that the specificities of the C-type CRDs are not only exclusively specified by the EPN or QPD motifs but also largely supported by other residues situated nearby in the binding site, as suggested by the MBP-A mutants [15]. In the present study, we have prepared another CEL-I mutant, in which Trp105 in the binding site of EPN-CEL-I was replaced by a histidine residue (EPNH-CEL-I), to further develop an engineered CEL-I with enhanced mannose specificity. X-ray crystallographic analysis of the EPNH-CEL-I/mannose complex also revealed the mannose-recognition mechanism of EPNH-CEL-I.

2. Materials and methods

2.1. Materials

Oligonucleotides used in this study were purchased from Sigma-Aldrich. The plasmid vectors pTAC-2 and pET-3a were obtained from DynaExpress and Novagen, respectively. Polyamidoamine dendrimers (PDs) with 64 amino surface groups (ethylenediamine core, generation 4.0, M.W. 14,214) (amino-PD) were obtained from Sigma-Aldrich. All the other chemicals were of analytical grade for biochemical use. Carbohydrate-immobilized Cellufine (mannose-Cellufine and GalNAc-Cellufine) columns were prepared by attaching carbohydrates to Cellufine gels (JNC Corp., Tokyo, Japan) using the cross-linking reagent divinyl sulfone (Sigma-Aldrich), as described previously [10].

2.2. Expression and purification of the recombinant CEL-I

The gene for EPNH-CEL-I (Supplementary figure) was synthesized by polymerase chain reaction (PCR) using the EPN-CEL-I gene [19] as a template and the primers listed in Supplementary table. PCR amplification was performed using the primers W105H-F and W105H-R, which contained the mutation site His105, and the primers corresponding to the 5′- and 3′-ends of the EPN-CEL-I gene (CEL-I-F and CEL-I-R), which contained the restriction sites *Nde*I and *BamH*I. After amplification of the 5′-terminal and 3′-terminal DNA fragments using combinations of the primers CEL-I-F/W105H-R and W105H-F/CEL-I-R, the fragments were ligated and amplified using CEL-I-F and CEL-I-R in a similar manner as that reported previously for EPN-CEL-I [19]. The resulting DNA encoding EPNH-CEL-I was cloned into *Escherichia coli* JM109 cells using the pTAC2 vector. The inserted EPNH-CEL-I gene was digested with the restriction enzymes *Nde*I and *Bam*HI and then ligated with the pET-3a vector previously digested with the same enzymes. The resulting plasmid was introduced into *E. coli* BL21(DE3)pLysS cells (Novagen), and expression of the protein was induced with 0.4 mM isopropylthiogalactoside. Because the recombinant proteins were obtained as inclusion bodies after disrupting the cells by sonication, they were solubilized in the solubilization buffer [50 mM Tris–HCl, pH 8.0; 0.2 M NaCl; 1 mM ethylenediamine tetraacetate (EDTA); and 6 M guanidine hydrochloride] and the protein was refolded in the refolding buffer (0.1 M Tris–HCl, pH 8.0; 0.4 M L-arginine; 2 mM EDTA; 5 mM reduced glutathione; 0.5 mM oxidized glutathione; and 0.1 mM phenylmethylsulfonyl fluoride). After dialysis of the refolded proteins in Tris-buffered saline (TBS; 10 mM Tris–HCl, pH 7.5; 0.15 M NaCl) containing 10 mM $CaCl_2$, the protein was purified by affinity chromatography

using the mannose-Cellufine column (3 × 10 cm). Wild-type- (WT-) and EPN-CEL-I were also expressed in an essentially similar manner, although purification was performed using GalNAc-Cellufine (for WT-CEL-I) or ion-exchange chromatography (for EPN-CEL-I) [19].

2.3. N-Terminal amino acid sequence analysis

The N-terminal amino acid sequence of the expressed protein was determined using a protein sequencer, PPSQ-21 (Shimadzu, Kyoto, Japan).

2.4. Circular dichroism (CD) measurements

Far-UV CD measurements of the proteins were performed within the range of 200–250 nm using a J-720 spectropolarimeter (JASCO). The spectra were measured using a quartz cell of 1-mm path length at 20°C in TBS containing 10 mM $CaCl_2$.

2.5. Measurement of carbohydrate-binding activity using sugar-PDs

Mannan and mannotriose were prepared as reported previously [20]. Sugar-PDs containing mannan or mannotriose were prepared by a reductive amination reaction between an aldehyde group of the sugars and primary amino groups of amino-PD, as described previously [21]; carbohydrates (110 μM) were incubated with amino-PD (0.17 μM) in 1 ml of 0.2 M sodium phosphate buffer (pH 8.0) in the presence of 110 μM $NaBH_3CN$ for 24 h at 45°C. The solution was then dialyzed against water to remove the residual reagents, and the resulting sugar-PDs were collected after freeze-drying. The carbohydrate-binding ability was evaluated by the increase in Rayleigh scattering on the basis of the complex formation between the lectin and sugar-PD. After recording the initial scattering intensity of the lectin solution at 420 nm (20 μg/ml, 1 ml) in TBS containing 10 mM $CaCl_2$ using a fluorescence spectrophotometer (Hitachi F-3010) at 25°C, small volumes of the sugar-PD solution in the same buffer were serially added, and the changes in the scattering intensity were recorded. Values were corrected for dilution by the addition of the sugar-PD solution. For the competitive experiments, various sugars were added to the pre-formed complex between EPNH-CEL-I (25 μg/mL) and mannotriose-PD (1.2 μg/mL). Dissociation of the EPNH-CEL-I/mannotriose-PD complex was evaluated by the changes in the light scattering intensity at 420 nm.

2.6. Isothermal titration calorimetry (ITC)

ITC for analyzing the interaction between EPNH-CEL-I and mannose was performed at 25°C using iTC 200 (MicroCal iTC200, GE Healthcare). Aliquots of the mannose solution (3.8 mM) were injected into the EPNH-CEL-I (6.1 mg/ml, 0.19 mM) solution in TBS containing 10 mM $CaCl_2$. The data were analyzed using ORIGIN software, version 7.0.

2.7. Glycoconjugate microarray analysis

Binding specificities of WT-CEL-I and EPNH-CEL-I for various glycoconjugates were examined by glycoconjugate microarray analysis, as described previously [22]. In brief, Cy3-labeled lectins were incubated overnight with the microarray, on which various glycoconjugates had been immobilized, in TBS containing 10 mM $CaCl_2$. After washing with the same buffer, the fluorescence intensity of the bound lectins was recorded.

2.8. Crystallization and X-ray crystallographic analysis of the EPNH-CEL-I/mannose complex

EPNH-CEL-I was crystallized by the hanging-drop and sitting-drop vapor diffusion methods. The initial screening was performed using the screening kits Crystal Screen 1 and 2 (Hampton Research, Aliso Viejo, CA, USA) and Wizard I and II (Emerald BioSystems, Inc., Bedford, MA, USA). In the initial screening of crystallization, 1 μl of the protein solution (10 mg/ml) in TBS containing 10 mM $CaCl_2$ was mixed with an equal volume of reservoir solution and allowed to equilibrate against 100 μl of the reservoir solution at 20°C. X-ray diffraction data were collected at −140°C using the Rigaku MicroMax-007 HF/Raxis IV++ System. Data indexing, integration, and scaling were performed with the CCP4 [23] programs Mosflm [24] and SCALA [25]. Data collection statistics are summarized in Table 1. All the data sets belonged to the $P2_1$ space group, with two EPNH-CEL-I molecules per asymmetric unit. The structures of the EPNH-CEL-I/mannose complex were determined by the molecular replacement method using native CEL-I (PDB ID: 1WMY) [12] as the search model. Molecular replacement was performed using the program Phaser [26]. The model was refined using the program Refmac [27] from the CCP4 suite. Manual fitting of the model was performed by the program Coot [28]. The quality of the final model was assessed by Ramachandran plot and the

program Procheck [29]. The refinement statistics are summarized in Table 1. Figures illustrating the protein models were prepared by PyMOL [30].

2.9. Affinity chromatography of CEL-I mutants having different amino acid residues at position 105

Genes for two additional EPN-CEL-I mutants, in which Trp105 was replaced by tyrosine (EPNY-CEL-I) or alanine (EPNA-CEL-I), were prepared using the QuikChange site-directed mutagenesis kit (Agilent, Santa Clara, CA) using the primers listed in Supplementary Table and the pET-3a vector containing the EPN-CEL-I gene as a template. Expression and refolding were performed in the same manner as those for EPNH-CEL-I. The resulting mutants, as well as WT-, EPN-, and EPNH-CEL-I, were applied to mannose-Cellufine and GalNA-Cellufine columns (2 × 2 cm) in TBS containing 10 mM $CaCl_2$, and after washing the columns with the same buffer, adsorbed proteins were eluted with TBS containing 20 mM EDTA.

3. Results

3.1. Expression and purification of EPNH-CEL-I

Figure 1 shows the structures of the carbohydrate-binding sites of CEL-I/N-acetylgalactosamine and MBP-A/methyl α-D-mannoside complexes as examples for galactose- and mannose-specific C-type lectins, respectively [12, 31]. They exhibit completely different specificities toward galactose and mannose despite possessing very similar structures around Ca^{2+}. This can be partly explained by the recognition of the orientation of 4-hydroxy groups (axial in galactose and equatorial in mannose) by the QPD or EPN motifs. However, even after changing the motif to EPN, the mutant CEL-I (EPN-CEL-I) showed very weak affinity, suggesting that additional interactions by other residue(s) are necessary for the recognition of mannose [19]. Therefore, we tried to replace Trp105 in CEL-I with a histidine residue on the basis of the comparison with MBP-A. The gene for the mutant CEL-I (EPNH-CEL-I) was synthesized by PCR using the primers containing the mutation site His105, as described in the Materials and methods. Because the expressed protein was recovered in inclusion bodies, they were refolded after complete unfolding using guanidine hydrochloride. After the refolding process, EPNH-CEL-I was purified by affinity chromatography using a sugar-immobilized column. Although WT-CEL-I can be purified using the GalNAc-Cellufine column, EPNH-CEL-I was not able to bind to

GalNAc-Cellufine (Fig. 2A). However, it could successfully bind to the mannose-Cellufine column and be eluted with EDTA (Fig. 2B). The purified protein showed single bands at 16 kDa and 32 kDa in the presence and absence of 2-mercaptoethanol, respectively (Fig. 2C), corresponding to the monomer and dimer linked by a disulfide bond. These results suggested that the expressed protein was correctly folded to adopt the native protein-like dimer structure with a Ca^{2+}-dependent mannose-binding ability. N-terminal amino acid analysis confirmed the sequence of the first five residues (Met-Asn-Gln-X-Pro) of the purified protein, indicating that the initiator methionine residue remained attached to the N-terminus in the recombinant protein. The unidentified residue X was assumed to be a cysteine (or half-cystine) residue from the designed sequence. To examine the secondary structure, the far-UV CD spectrum of the purified EPNH-CEL-I was measured along with that of WT-CEL-I. As shown in Fig. 3. EPNH-CEL-I showed a CD spectrum with a broad negative peak around the region of 210–240 nm, which is similar to that of WT-CEL-I, confirming that EPNH-CEL-I had a correctly folded structure. However, a slight difference in the intensity was also observed between the 205–220-nm and 220–240-nm regions. This may be caused by the replacement of a tryptophan residue (Trp105), which has a large UV absorption around this region, by a histidine residue.

3.2. Carbohydrate-binding specificity of EPNH-CEL-I

Binding abilities of EPNH-CEL-I for different sugars were examined by an assay using sugar-PD containing reducing sugar attached to the primary amino groups at the surface of PD [21]. Figure 4A shows the change in the light-scattering intensity measured at 420 nm. When mannan-PD was added to the solutions of WT-CEL-I, EPN-CEL-I, or EPNH-CEL-I, EPNH-CEL-I showed a large increase in the light-scattering intensity at 420 nm, while EPN-CEL-I showed a slight increase and WT-CEL-I showed a very little change. These results suggest that EPNH-CEL-I has a significant binding affinity for mannose, although EPN-CEL-I also has a weak affinity. To compare the affinities for different sugars, a competitive assay for binding of EPNH-CEL-I with mannotriose-PD was conducted as shown in Fig. 4B. After the formation of a complex between EPN-CEL-I and mannotriose-PD, several simple carbohydrates were added to compete for binding to the protein. Consequently, the strongest binding was observed for mannose and methyl α-D-mannoside, confirming its definite affinity for mannose and its related carbohydrates. Glucose and maltose also showed moderate affinity for EPNH-CEL-I because glucose has the same configuration of 3- and 4-hydroxy groups as mannose. It seems interesting that EPNH-CEL-I still retained a considerable degree of affinity for N-acetylgalactosamine,

while galactose showed a very weak affinity. This suggests that the acetamido group of N-acetylgalactosamine has significant interactions with the carbohydrate-binding site in EPNH-CEL-I. As shown in Fig. 5, the binding constant and thermodynamic parameters for the binding of mannose with EPNH-CEL-I were evaluated by ITC measurement as follows: binding stoichiometry (N) = 2.14 ± 0.0858, association constant (K_a) = $3.17 \times 10^3 \pm 399$ M^{-1}, enthalpy change (ΔH) = $-3.41 \times 10^3 \pm 218$ J/mol, and entropy change (ΔS) = 55.7 J/mol/K. These values indicate that EPNH-CEL-I has two binding sites and shows an affinity for mannose comparable to that of common lectins. However, the attempts to measure the binding constants for other sugars were unsuccessful, probably because their affinities were too weak to be evaluated under the current conditions.

Carbohydrate-binding specificities of EPNH-CEL-I for various larger oligosaccharides were examined by glycoconjugate array analysis [22, 32] in comparison with those of WT-CEL-I. Figure 6 demonstrates the binding of the Cy3-labeled lectins to the microarray, on which various glycoproteins and glycopolymers were immobilized. Glycoconjugates showing a relatively high affinity for these proteins are listed in Table 2. WT-CEL-I strongly bound to several glycoconjugates such as bovine submaxillary mucin (BSM), GalNAcα1-3Galβ1-PAA (polyacrylamide) (A-di), GalNAcα1-PAA (Tn), GalNAcα1-3GalNAcβ1-PAA (Forssman), and GalNAcβ1-3GalNAcβ1-PAA (di-GalNAcβ). These glycoconjugates contain galactose and/or N-acetylgalactosamine (Table 2). As we reported previously, CEL-I is highly specific to N-acetylgalactosamine, particularly disaccharides containing N-acetylgalactosamine at the nonreducing end [10, 12, 33]. Thus, the results of glycoconjugate array analysis confirmed such previous observations. The highest binding affinity for BSM may be a result of the effect of clustering of the carbohydrate chains protruding on the surface of BSM, which may enhance the avidity of the lectin. In contrast, while EPNH-CEL-I exhibited the highest affinity for di-GalNAcβ, its binding profile for various glycoconjugates was considerably different from that of WT-CEL-I. The affinity of EPNH-CEL-I for ovalbumin (OVA), invertase (INV), and mannan from *Candida albicans* (Mannan CA), which mainly contain terminal mannose, significantly increased, whereas that for A-di, Tn, Forssman, BSM, and aGal, which contain terminal N-acetylgalactosamine or galanctose, decreased. It is also conspicuous that EPNH-CEL-I showed a relatively high affinity for [3S]Le^a and di-GalNAcβ. The increase in the affinity for the former could be attributed to its sulfated galactose structure that may have induced a favorable interaction with EPNH-CEL-I; however, the reason for a higher affinity for di-GalNAcβ remains unclear. It may partly be because of its disaccharide GalNAc structure, considering the observation that GalNAc still showed some extent of affinity for EPNH-CEL-I (Fig. 4B), although it was insufficient to bind to GalNAc-Cellufine columns

(Fig. 2A).

3.3. X-ray crystallographic analysis of the EPNH-CEL-I/mannose complex

To elucidate the mechanism of mannose recognition, EPNH-CEL-I complexed with mannose was crystallized and its tertiary structure was determined by X-ray crystallographic analysis. The crystals were obtained at 20°C in the buffer containing polyethyleneglycol as a precipitant (0.2 M magnesium acetate; 0.1 M sodium cacodylate, pH 6.5; and 30% polyethyleneglycol 4000). The crystal showed X-ray diffraction up to 1.7 Å resolution, and the structure was determined by the molecular replacement method using native CEL-I as a search model. As shown in Fig. 7A, during the course of model refinement, a distinct electron density corresponding to the bound mannose was observed in the vicinity of the Ca^{2+} ion in the binding site. Therefore, further refinement was performed including a model of mannose fitted to each binding site. Statistics of the diffraction data collection and the refinement parameters are summarized in Table 1. The entire structure of the EPNH-CEL-I/mannose complex is shown in Fig. 7B with that of native CEL-I superposed. As shown in this figure, the overall structure of EPNH-CEL-I is similar to that of native CEL-I. Figure 8 shows the structures of the carbohydrate-binding sites EPNH-CEL-I, native CEL-I, and MBP-A. In these models, bound sugars are recognized through coordinate bonds with Ca^{2+} ions and hydrogen bond networks with nearby residues. As shown in Fig. 8A and B, two different orientations of bound mannose related by 180° rotation were observed in the EPNH-CEL-I/mannose complex, suggesting that both orientations can be readily accommodated in the same binding site, although the orientation of mannose in Fig. 8B was only found in one of the four subunits in the asymmetric unit of the crystal. The two possible orientations of mannose are enabled by the fact that the directions of the 3- and 4-hydroxy groups of mannose can be the same in both cases, when hydrogen bonds are formed with the surrounding residues Glu101, Asn103, Glu109, and Asn123. This also suggests that specific interactions are not present between mannose and the residues other than these four residues, although one hydrogen bond between the 1- or 2-hydroxy group and Arg115 was observed. Such a binding of mannose in alternative orientations has also been observed for MBP-A and MBP-C with bound mannose oligosaccharides, depending on their α-glycosidic linkages [31, 34]. In case of the CEL-I/N-acetylgalactosamine complex (Fig. 8C), there are additional interactions responsible for a high N-acetylgalactosamine specificity: two hydrogen bonds of the acetamide group of N-acetylgalactosamine with Arg115 in addition to a van der Waals contact with Gln70 [12]. In addition, Trp105 contributes to

a hydrophobic interaction with the apolar face of N-acetylgalactosamine to stabilize the binding. In the EPNH-CEL-I/mannose complex, the replacement of QPD by EPN caused the switch of the donor/acceptor combination of hydrogen bonds, leading to preferable bonding of hydrogen with the 3- or 4-hydroxy group of mannose rather than the 4-hydroxy group of N-acetyl-galactosamine or galactose, as shown in Fig. 8A and B. In case of EPNH-CEL-I, the binding of mannose is further stabilized by His105, which is more hydrophilic than the tryptophan residue and is therefore more suitable in the interaction with mannose. This also coincides with the fact that there is no difference in the affinity between mannose and methyl α-D-mannoside for EPNH-CEL-I, as shown by the inhibition assay using sugar-PD (Fig. 4). Figure 8D shows the comparison of binding modes of mannose in EPNH-CEL-I and methyl α-D-mannoside in MBP-A. As shown in this figure, the relative positions of mannose and methyl α-D-mannoside are very similar, although the distance between His105 and mannose in EPNH-CEL-I is slightly larger than that between His189 and methyl α-D-mannoside in MBP-A.

3.4. Effects of the residues at position 105 on binding specificity

As revealed by X-ray crystallographic analysis, EPNH-CEL-I was found to have a higher affinity for mannose by stabilizing the binding with histidine instead of tryptophan in native CEL-I. This suggests that the nature of the residue at position 105 has close relationships with binding specificity. To examine this further, we prepared two additional mutants of CEL-I, i.e., EPNY- and EPNA-CEL-I, which contain Tyr105 and Ala105, respectively. The specificities of these mutants were evaluated by affinity chromatography on mannose- and GalNAc-Cellufine columns. As shown in Fig. 9, when these mutant proteins as well as WT-, EPN-, and EPNH-CEL-I were applied to these columns, mannose-binding affinity was observed in the case of EPNY-, EPNH-, and EPNA-CEL-I. On the other hand, affinity for GalNAc-Cellufine was observed in the case of WT-, EPN-, and EPNY-CEL-I. These results suggest that Tyr105 and Ala105 are available for proper interaction with mannose beside His105. However, EPNY-CEL-I also showed a significant affinity for GalNAc, which is probably because of the moderate hydrophobic nature of tyrosine. These results support the assumption that the hydrophobicity of the residue at position 105 is important for distinguishing between galactose and mannose.

4. Discussion

The C-type CRDs show similar folding, regardless of their diverse carbohydrate specificities [3]. They share a common domain architecture consisting of the core region with two α-helices and several β-strands and a long loop that determines the binding specificities for carbohydrates. This long loop can be more diverse in the C-type lectin-like domains (CTLDs), which adopt structures similar to the C-type CRDs but interact with other molecules such as proteins, lipids, and inorganic molecules such as $CaCO_3$ and water [35]. Such structural features make the C-type CRD and CTLD versatile modules for the recognition of various molecules in important biological processes. The QPD and EPN motifs are located in this long loop region constituting part of the carbohydrate-binding site and have been known to be important characteristics to predict the binding specificity for galactose- or mannose-related carbohydrates. These three amino acids are directly involved in the binding of both Ca^{2+} and carbohydrates by forming coordinate bonds and hydrogen bonds. In this binding model, the combinations of Glu/Asn in EPN or Gln/Asp in QPD are very important for determining the orientation of the hydroxy group of bound carbohydrates. This has been experimentally proven by the mutagenesis of MBP-A [14, 15], in which the EPN motif in MBP-A was replaced by QPD. The resulting mutant showed a relatively weak affinity for galactose. Further mutation to introduce a tryptophan residue that forms hydrophobic stacking with the apolar face of galactose led to a much higher affinity for galactose, thereby demonstrating the importance of a hydrophobic contact between an aromatic residue and galactose. The importance of hydrophobic stacking in the recognition of galactose has also been shown for various galactose-binding lectins, including the other *C. echinata* lectins CEL-III [36] and CEL-IV [37]. Interestingly, CEL-IV shows galactose specificity, although it contains an EPN motif in the carbohydrate-binding site. This discrepancy was explained by the crystal structure of CEL-IV complexed with galactose-containing carbohydrates, in which the aromatic residue Trp79 specifies the orientation of the bound galactose by stacking interaction so that EPN can form proper hydrogen bonds with galactose [37].

We have previously shown that the mutation from the EPN to QPD motif of CEL-I leads to mannose specificity, whereas the affinity of the mutant EPN-CEL-I for mannose is so weak that it cannot bind to the GalNAc-immobilized affinity column [19]. As demonstrated in this study, mannose specificity was found to be significantly enhanced by the introduction of a histidine residue instead of Trp105. This result suggests the importance of the nature of amino acids that stabilize bound carbohydrates by nonspecific interactions; the hydrophilic nature of histidine seems to be suitable for the stabilization of mannose that lacks an apolar face in contrast to galactose. This has been further

supported by affinity chromatography of the two additional mutants EPNY- and EPNA-CEL-I (Fig. 9). Although EPNY-CEL-I exhibited affinity for both mannose and N-acetylgalactosamine, EPNA-CEL-I only bound to the mannose column, similar to EPNH-CEL-I. These results strongly suggest that the hydrophobicity of the residue stabilizing the orientation of the bound sugars significantly influences binding specificities; a more hydrophobic nature is favorable for the binding of galactose.

Although EPNH-CEL-I did not bind to the GalNAc-Cellufine column, some degree of affinity for N-acetylgalactosamine was observed in the inhibition experiments (Fig. 4B). As revealed by X-ray crystallographic analysis [12], native CEL-I shows strong N-acetylgalactosamine specificity through two hydrogen bonds with Arg115 and van der Waals interaction with Gln70 (Fig. 8C). Therefore, possibly, N-acetylgalactosamine can also bind to EPNH-CEL-I with moderate affinity through these interactions with Arg115 and Gln70. Glycoconjugate microarray analysis also proved definite affinity for N-acetyl-galactosamine-containing oligosaccharides with an even higher intensity than that for mannose-containing oligosaccharides. This may be due to additional interactions with the oligosaccharides rather than with the N-acetylgalactosamine monosaccharide. In the EPNH-CEL-I/mannose complex, Arg115 was found to form a hydrogen bond with the 1- or 2-hydroxy group of mannose in different conformations (Fig. 8A and B), depending on two alternative orientations of the bound mannose, suggesting that Arg115 has some extent of contribution in mannose recognition by EPNH-CEL-I. In the competition assay using sugar-PD (Fig. 4), glucose also exhibited a moderately high affinity for EPNH-CEL-I. As apparent from Fig. 8A, the 2- and 6-hydroxy groups of mannose are not necessary for the binding to EPNH-CEL-I, while the 3- and 4-hydroxy groups are essential. Therefore, it seems reasonable that glucose, which has the same configuration regarding 3- and 4-hydroxy groups as mannose, can bind to EPNH-CEL-I with a moderate affinity. Along with the findings of the preceding studies on engineering of MBP-A to change its specificity to galactose binding [14, 15] and its applications for the identification of cell surface glycoconjugates [38-40], a reversal change in the specificity of CEL-I from galactose (N-acetylgalactosamine) to mannose shown in the present study suggests the versatility of C-type CRDs. As observed in glycoconjugate microarray analysis, mutations in CEL-I seem to have affected the recognition of not only monosaccharides but also oligosaccharides. Such alterations in the recognition of oligosaccharides or glycolipids have also been reported for other C-type lectins [31, 41, 42], which may involve interaction with additional sites of protein (subsites) extending from the primary binding site containing Ca^{2+}. The versatility of C-type CRDs appears to be closely related to the structural features of the C-type CRDs that are composed of two parts: a stable core structure with a common fold and a

long loop region that can potentially accommodate various molecules. The binding of CTLDs to various molecules strongly suggests that their molecular architecture could be useful in the development of novel molecular recognition proteins.

Acknowledgments

We are grateful to Ms. Jinko Murakami and Ms. Keiko Hiemori for help in glycoconjugate microarray analysis. This work was supported by a Grants-in-Aid for Scientific Research (C) to TH (26450128) and Grants-in-Aid for Young Scientists (B) to HU (10452872) and SG (00346587) from the Japan Society for the Promotion of Science (JSPS).

References

[1] K. Drickamer, Two distinct classes of carbohydrate-recognition domains in animal lectins, J Biol Chem, 263 (1988) 9557-9560.

[2] D.C. Kilpatrick, Animal lectins: a historical introduction and overview., Biochim Biophys Acta, 1572 (2002) 187-197.

[3] A.N. Zelensky, J.E. Gready, The C-type lectin-like domain superfamily., FEBS J, 272 (2005) 6179-6217.

[4] S. Mukherjee, H. Zheng, M.G. Derebe, K.M. Callenberg, C.L. Partch, D. Rollins, D.C. Propheter, J. Rizo, M. Grabe, Q.X. Jiang, L.V. Hooper, Antibacterial membrane attack by a pore-forming intestinal C-type lectin, Nature, 505 (2014) 103-107.

[5] E. Riboldi, R. Daniele, C. Parola, A. Inforzato, P.L. Arnold, D. Bosisio, D.H. Fremont, A. Bastone, M. Colonna, S. Sozzani, Human C-type lectin domain family 4, member C (CLEC4C/BDCA-2/CD303) is a receptor for asialo-galactosyl-oligosaccharides., J Biol Chem, 286 (2011) 35329-35333.

[6] D. Mourão-Sá, M.J. Robinson, S. Zelenay, D. Sancho, P. Chakravarty, R. Larsen, M. Plantinga, N. Van Rooijen, M.P. Soares, B. Lambrecht, C. Reis e Sousa, CLEC-2 signaling via Syk in myeloid cells can regulate inflammatory responses., Eur J Immunol, 41 (2011) 3040-3053.

[7] D.C. Kilpatrick, Mannan-binding lectin and its role in innate immunity., Transfus Med, 12 (2002) 335-352.

[8] A. Cambi, C.G. Figdor, Dual function of C-type lectin-like receptors in the immune system, Curr Opin Cell Biol, 15 (2003) 539-546.

[9] F. Liu, J. Li, J. Fu, Y. Shen, X. Xu, Two novel homologs of simple C-type lectin in grass carp (*Ctenopharyngodon idellus*): Potential role in immune response to bacteria., Fish Shellfish Immunol, 31 (2011) 765–773.

[10] T. Hatakeyama, H. Kohzaki, H. Nagatomo, N. Yamasaki, Purification and characterization of four Ca^{2+}-dependent lectins from the marine invertebrate, *Cucumaria echinata*., J Biochem, 116 (1994) 209-214.

[11] H. Unno, S. Goda, T. Hatakeyama, Hemolytic lectin CEL-III heptamerizes via a large structural transition from α-helices to a β-barrel during the transmembrane pore formation process, J Biol Chem, 289 (2014) 12805-12812.

[12] H. Sugawara, M. Kusunoki, G. Kurisu, T. Fujimoto, H. Aoyagi, T. Hatakeyama, Characteristic recognition of N-acetylgalactosamine by an invertebrate C-type Lectin, CEL-I, revealed by X-ray

crystallographic analysis., J Biol Chem, 279 (2004) 45219-45225.

[13] T. Hatakeyama, K. Ohuchi, M. Kuroki, N. Yamasaki, Amino acid sequence of a C-type lectin CEL-IV from the marine invertebrate *Cucumaria echinata*, Biosci Biotech Biochem, 59 (1995) 1314-1317.

[14] K. Drickamer, Engineering galactose-binding activity into a C-type mannose-binding protein., Nature, 360 (1992) 183-186.

[15] A.R. Kolatkar, A.K. Leung, R. Isecke, R. Brossmer, K. Drickamer, W.I. Weis, Mechanism of N-acetylgalactosamine binding to a C-type animal lectin carbohydrate-recognition domain., J Biol Chem, 273 (1998) 19502-19508.

[16] S.T. Iobst, K. Drickamer, Binding of sugar ligands to Ca^{2+}-dependent animal lectins. II. Generation of high-affinity galactose binding by site-directed mutagenesis., J Biol Chem, 269 (1994) 15512-15519.

[17] Y. Ogasawara, D.R. Voelker, Altered carbohydrate recognition specificity engineered into surfactant protein D reveals different binding mechanisms for phosphatidylinositol and glucosylceramide, J Biol Chem, 270 (1995) 14725-14732.

[18] F.X. McCormack, Y. Kuroki, J.J. Stewart, R.J. Mason, D.R. Voelker, Surfactant protein A amino acids Glu195 and Arg197 are essential for receptor binding, phospholipid aggregation, regulation of secretion, and the facilitated uptake of phospholipid by type II cells, J Biol Chem, 269 (1994) 29801-29807.

[19] T. Hatakeyama, T. Ishimine, T. Baba, M. Kimura, H. Unno, S. Goda, Alteration of the Carbohydrate-Binding Specificity of a C-type Lectin CEL-I Mutant with an EPN Carbohydrate-Binding Motif, Protein Pept Lett, 20 (2013) 796-801.

[20] Y. Kato, K. Kochi, H. Unno, S. Goda, T. Hatakeyama, Manno-oligosaccharide-binding ability of mouse RegIV/GST-fusion protein evaluated by complex formation with the carbohydrate-containing polyamidoamine dendrimer, Biosci Biotechnol Biochem, (2014) 1-4.

[21] T. Hatakeyama, R. Karino, Y. Terai, M. Kimura, H. Unno, S. Goda, An assay for carbohydrate-binding activity of lectins using polyamidoamine dendrimer conjugated with carbohydrates, Biosci Biotechnol Biochem, 76 (2012) 1999-2001.

[22] H. Tateno, A. Mori, N. Uchiyama, R. Yabe, J. Iwaki, T. Shikanai, T. Angata, H. Narimatsu, J. Hirabayashi, Glycoconjugate microarray based on an evanescent-field fluorescence-assisted detection principle for investigation of glycan-binding proteins, Glycobiology, 18 (2008) 789-798.

[23] N. Collaborative Computational Project, The CCP4 suite: programs for protein crystallography,

Acta Crystallogr. D Biol. Crystallogr., 50 (1994).

[24] A.G. Leslie, The integration of macromolecular diffraction data, Acta Crystallogr D Biol Crystallogr, 62 (2006) 48-57.

[25] P. Evans, Scaling and assessment of data quality, Acta Crystallogr D Biol Crystallogr, 62 (2006) 72-82.

[26] A.J. McCoy, R.W. Grosse-Kunstleve, L.C. Storoni, R.J. Read, Likelihood-enhanced fast translation functions, Acta Crystallogr D Biol Crystallogr, 61 (2005) 458-464.

[27] G.N. Murshudov, A.A. Vagin, E.J. Dodson, Refinement of macromolecular structures by the maximum-likelihood method, Acta Crystallogr D Biol Crystallogr, 53 (1997) 240-255.

[28] P. Emsley, B. Lohkamp, W.G. Scott, K. Cowtan, Features and development of Coot, Acta Crystallogr D Biol Crystallogr, 66 (2010) 486-501.

[29] R. Laskowski, M. MacArthur, D. Moss, J. Thornton, *PROCHECK*: a program to check the stereochemical quality of protein structures, J. Appl. Crystallogr., 26 (1993) 283–291.

[30] W.L. DeLano, The PyMOL Molecular Graphics Systems, DeLano Scientific, San Carlos, CA, 2002.

[31] K.K. Ng, A.R. Kolatkar, S. Park-Snyder, H. Feinberg, D.A. Clark, K. Drickamer, W.I. Weis, Orientation of bound ligands in mannose-binding proteins. Implications for multivalent ligand recognition., J Biol Chem, 277 (2002) 16088-16095.

[32] H. Tateno, Evaluation of glycan-binding specificity by glycoconjugate microarray with an evanescent-field fluorescence detection system, Methods Mol Biol, 1200 (2014) 353-359.

[33] T. Hatakeyama, K. Shiba, N. Matsuo, T. Fujimoto, T. Oda, H. Sugawara, H. Aoyagi, Characterization of recombinant CEL-I, a GalNAc-specific C-type lectin, expressed in *Escherichia coli* using an artificial synthetic gene., J Biochem, 135 (2004) 101-107.

[34] K.K. Ng, K. Drickamer, W.I. Weis, Structural analysis of monosaccharide recognition by rat liver mannose-binding protein., J Biol Chem, 271 (1996) 663-674.

[35] K. Drickamer, C-type lectin-like domains., Curr Opin Struct Biol, 9 (1999) 585-590.

[36] T. Hatakeyama, H. Unno, Y. Kouzuma, T. Uchida, S. Eto, H. Hidemura, N. Kato, M. Yonekura, M. Kusunoki, C-type lectin-like carbohydrate recognition of the hemolytic lectin CEL-III containing ricin-type -trefoil folds., J Biol Chem, 282 (2007) 37826-37835.

[37] T. Hatakeyama, T. Kamiya, M. Kusunoki, S. Nakamura-Tsuruta, J. Hirabayashi, S. Goda, H. Unno, Galactose recognition by a tetrameric C-type lectin, CEL-IV, containing the EPN carbohydrate recognition motif., J Biol Chem, 286 (2011) 10305-10315.

[38] A.S. Powlesland, P.G. Hitchen, S. Parry, S.A. Graham, M.M. Barrio, M.T. Elola, J. Mordoh, A. Dell, K. Drickamer, M.E. Taylor, Targeted glycoproteomic identification of cancer cell glycosylation, Glycobiology, 19 (2009) 899-909.

[39] A.S. Powlesland, A. Quintero-Martinez, P.G. Lim, Z. Pipirou, M.E. Taylor, K. Drickamer, Engineered carbohydrate-recognition domains for glycoproteomic analysis of cell surface glycosylation and ligands for glycan-binding receptors, Methods Enzymol, 480 (2010) 165-179.

[40] A.S. Powlesland, M.M. Barrio, J. Mordoh, P.G. Hitchen, A. Dell, K. Drickamer, M.E. Taylor, Glycoproteomic characterization of carriers of the CD15/Lewisx epitope on Hodgkin's Reed-Sternberg cells, BMC Biochem, 12 (2011) 13.

[41] H. Wang, J. Head, P. Kosma, H. Brade, S. Müller-Loennies, S. Sheikh, B. McDonald, K. Smith, T. Cafarella, B. Seaton, E. Crouch, Recognition of heptoses and the inner core of bacterial lipopolysaccharides by surfactant protein d, Biochemistry, 47 (2008) 710-720.

[42] T.K. Carlson, J.B. Torrelles, K. Smith, T. Horlacher, R. Castelli, P.H. Seeberger, E.C. Crouch, L.S. Schlesinger, Critical role of amino acid position 343 of surfactant protein-D in the selective binding of glycolipids from *Mycobacterium tuberculosis*, Glycobiology, 19 (2009) 1473-1484.

[43] M. Shimokawa, A. Fukudome, R. Yamashita, Y. Minami, F. Yagi, H. Tateno, J. Hirabayashi, Characterization and cloning of GNA-like lectin from the mushroom *Marasmius oreades*, Glycoconj J, 29 (2012) 457-465.

Figure legends

Fig. 1. Comparison of the carbohydrate-binding sites of CEL-I and MBP-A. (A) CEL-I/N-acetylgalactosamine complex (PDB ID: 1WMY) [12]. (B) MBP-A/methyl α-D-mannoside complex (PDB ID: 1KWU) [31]. The coordinate bonds and hydrogen bonds are depicted by yellow dashed lines. The amino acid residues consisting of the QPD and EPN motifs are shown in red.

Fig. 2. Affinity chromatography of EPNH-CEL-I on the carbohydrate-immobilized Cellufine columns. Refolded EPNH-CEL-I was applied to the GalNAc-Cellufine column (A) or mannose-Cellufine column (B). After elution of the nonadsorbed proteins with TBS containing 10 mM $CaCl_2$, the adsorbed protein was eluted with TBS containing 20 mM EDTA. (C) SDS-PAGE of EPNH-CEL-I eluted from the mannose-Cellufine column indicated by the bar in *panel* B in the presence and absence of 2-mercaptoethanol (2-ME).

Fig. 3. Far-UV CD spectra of EPNH-CEL-I and WT-CEL-I. Measurement was performed with 0.28 mg/ml protein in TBS containing 10 mM $CaCl_2$ at 20°C. The values [θ] are expressed as the mean residue molar ellipticity.

Fig. 4. Carbohydrate-binding specificity of the lectins examined by complex formation with sugar-PD. (A) The changes in the light-scattering intensity induced by complex formation between the lectins and mannan-PD were measured using a fluorescence spectrophotometer at 25°C. (B) The solutions of indicated sugars were added to the pre-formed complex between EPNH-CEL-I and mannotriose-PD. Dissociation of the EPNH-CEL-I/mannotriose-PD complex was evaluated by the changes in the light scattering intensity. The initial light scattering intensity of the pre-formed complex was considered as 100%.

Fig. 5. ITC for the binding of mannose to EPNH-CEL-I. The mannose solution was titrated into a temperature-controlled sample cell containing the EPNH-CEL-I solution. The change in the heat accompanying the binding (*upper panel*) was integrated and plotted against the mannose/EPNH-CEL-I

molar ratio (*lower panel*).

Fig. 6. Glycoconjugate microarray analysis of WT-CEL-I and EPNH-CEL-I. The binding specificities of Cy3-labeled WT-CEL-I and EPNH-CEL-I for various glycoconjugates were measured. Glycoconjugates used in this analysis are designated by the abbreviations, as listed in ref. [43].

Fig. 7. The crystal structure of the EPNH-CEL-I/mannose complex. (A) The binding site with the bound mannose is shown with a 2*Fo-Fc* electron density map contoured at 1σ. (B) Main chain structure of the EPNH-CEL-I/mannose complex (*yellow*) is shown by a ribbon model in comparison with that of native CEL-I (*pink*).

Fig. 8. Comparison of the carbohydrate-binding sites of EPNH-CEL-I, native CEL-I, and MBP-A. (A and B) Two different binding modes of EPNH-CEL-I with the bound mannose rotated by 180°. (C) The binding site of the CEL-I/N-acetylgalactosamine complex [12]. (D) Comparison of the EPNH-CEL-I/mannose complex (*green*) with the MBP-A/methyl α-D-mannoside complex (*yellow*). Only residue numbers for the MBP-A/methyl α-D-mannoside complex are indicated.

Fig. 9. Affinity chromatography of WT and CEL-I mutants. Each protein was applied to mannose-Cellufine (*left panels*) or GalNAc-Cellufine (*right panels*) columns in TBS containing 10 mM $CaCl_2$. After washing the columns with the same buffer, bound proteins were eluted with TBS containing 20 mM EDTA at the positions indicated by vertical arrows.

Table 1

Diffraction statistics and refinement parameters of the EPNH-CEL-I/mannose complex crystal

Numbers in parentheses are for the highest shell.

Crystal type	EPNH-CEL-I/Man
Data collection and processing statistics	
Space group	$P2_1$
Unit cell dimension *a*, *b*, *c* (Å) *α*, *β*, *γ* (°)	*a* = 69.29, *b* = 61.06, *c* = 80.70 *α* = *γ* = 90.00, *β* = 109.39
Wavelength (Å)	1.5418
Resolution (Å)	30.53–1.70 (1.79–1.70)
Total reflection	231026
Unique reflection	60007
$I/\sigma I$	15.9 (3.9)
Redundancy	3.8 (3.8)
Completeness (%)	92.6 (88.6)
R_{merge} (%)	5.1 (30.0)
Refinement statistics	
R/R_{free} (%)	15.2/19.0
Root mean square deviation	
Bond length (Å)	0.019
Bond angles (°)	1.800

[a] $R_{merge} = 100\Sigma|I - \langle I \rangle|/\Sigma I$, where I is the observed intensity and $\langle I \rangle$ is the average intensity of multiple observations of symmetry-related reflections.

Table 2

Glycans showing significant affinity for WT-CEL-I and EPNH-CEL-I

Protein	Abbreviation	Structure
WT-CEL-I	A-di	GalNAcα1-3Galβ1-PAA
	di-GalNAcβ	GalNAcβ1-3GalNAcβ1-PAA
	Tn	GalNAcα1-PAA
	Forssman	GalNAcα1-3GalNAcβ1-PAA
	Asialo-BSM	Asialo bovine submaxillary mucin (Tn)
	BSM	Bovine submaxillary mucin (Sialyl Tn)
	aGal	Galα1-PAA
EPNH-CEL-I	[3S]Le[a]	($3OSO_3$)Galβ1-3(Fucα1-4)GlcNAcβ1-PAA
	di-GalNAcβ	GalNAcβ1-3GalNAcβ1-PAA
	Asialo-TG	Asialo porcine thyroglobulin (Desialylated complex-type N-glycans, high-mannose-type N-glycans)
	OVA	Ovoalbumin (Hybrid-type N-glycans)
	INV	Yeast invertase (High mannose-type N-glycans)
	Asialo-GP	Asialo human glycophorin MN (T)
	Mannan (CA)	*C. albicans* mannan

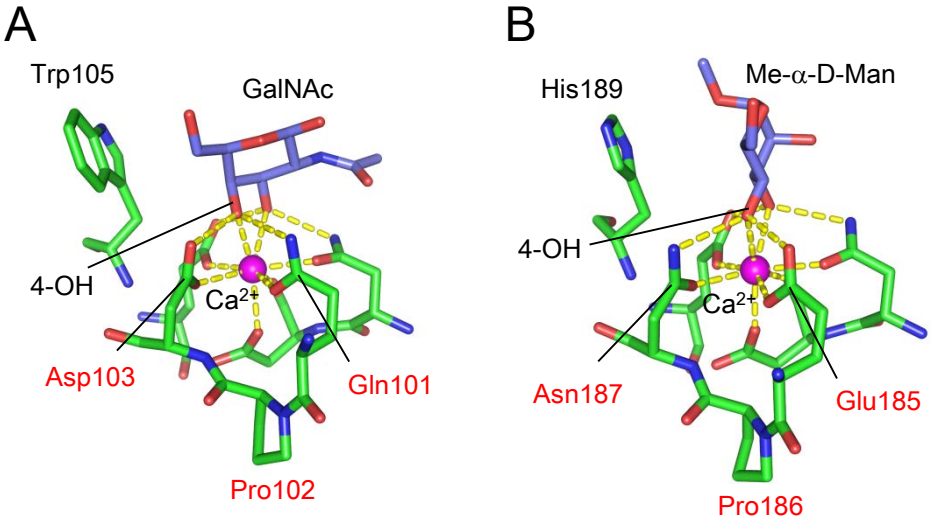
A
Trp105
GalNAc
4-OH
Ca2+
Asp103
Gln101
Pro102
B
His189
Me-α-D-Man
4-OH
Ca2+
Asn187
Glu185
Pro186

Fig. 1

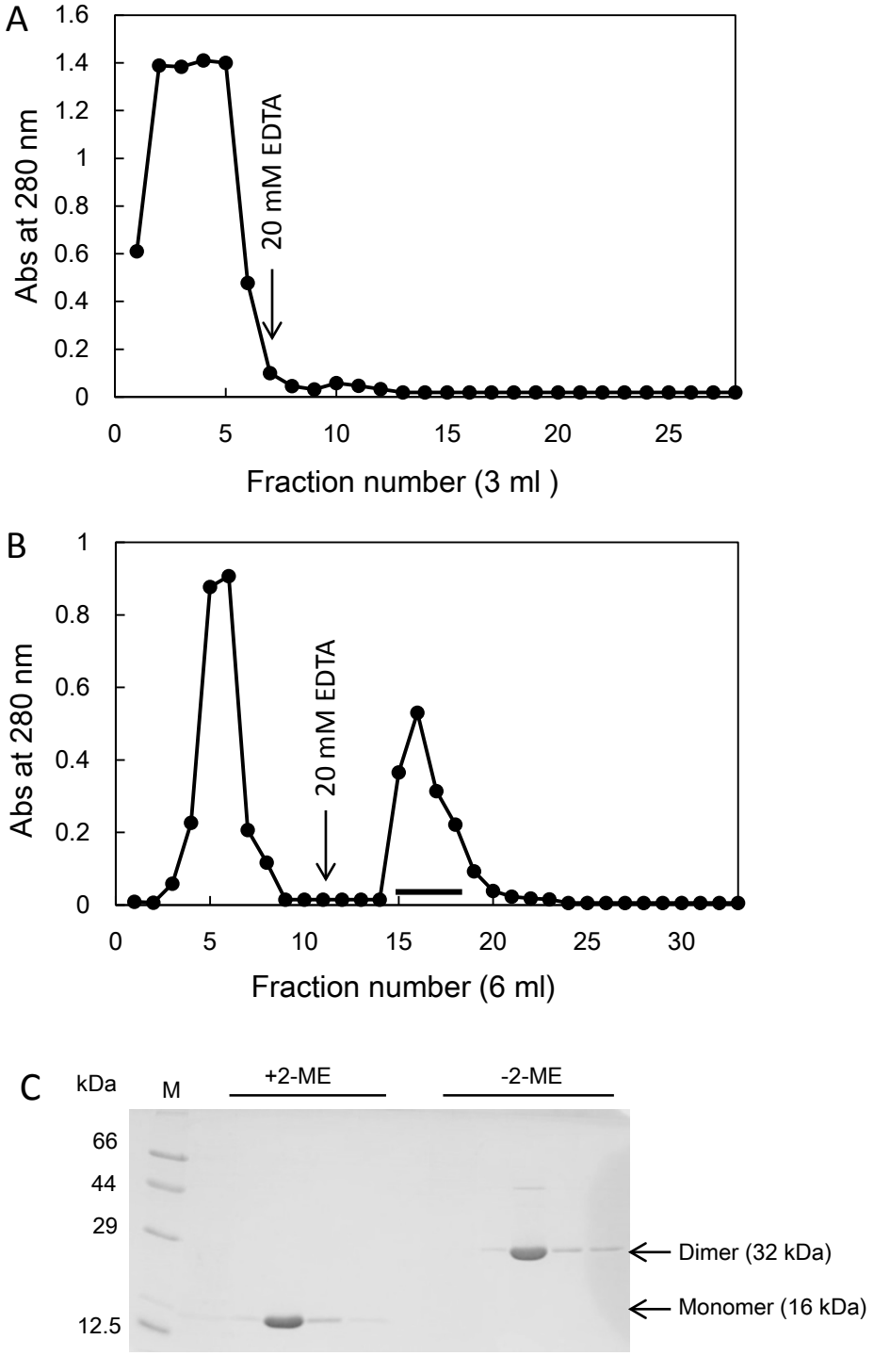
A
Abs at 280 nm
1.6
1.4
1.2
1
0.8
0.6
0.4
0.2
0
20 mM EDTA
0
5
10
15
20
25
Fraction number (3 ml)
B
Abs at 280 nm
1
0.8
0.6
0.4
0.2
0
20 mM EDTA
0
5
10
15
20
25
30
Fraction number (6 ml)
C
kDa
M
+2-ME
-2-ME
66
44
29
12.5
Dimer (32 kDa)
Monomer (16 kDa)

Fig. 2

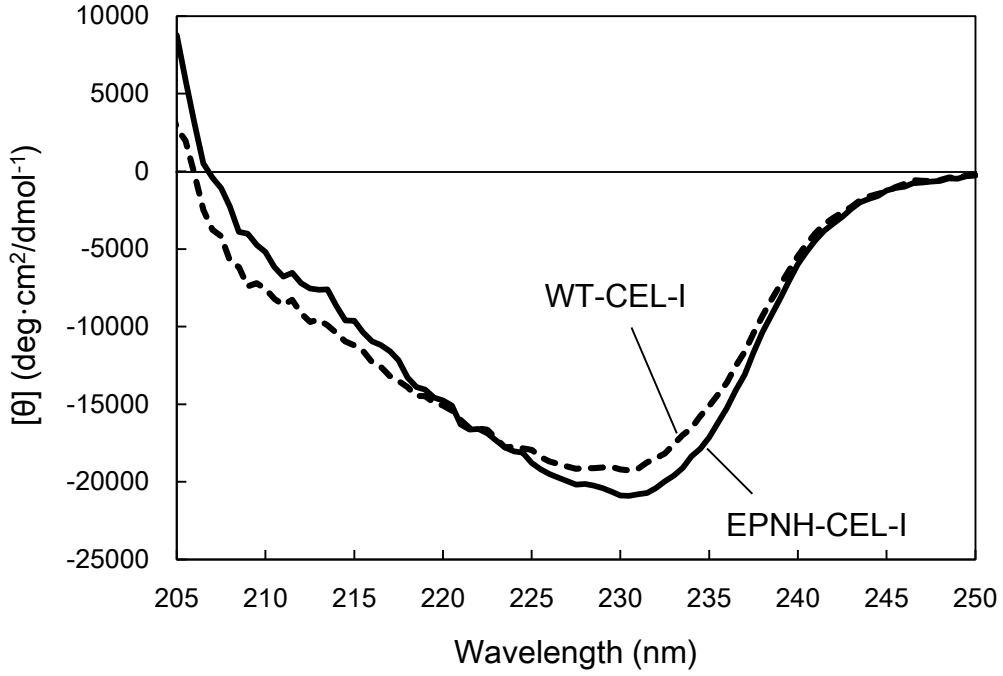
10000
5000
0
-5000
-10000
-15000
-20000
-25000
[θ] (deg·cm²/dmol⁻¹)
205
210
215
220
225
230
235
240
245
250
Wavelength (nm)
WT-CEL-I
EPNH-CEL-I

Fig. 3

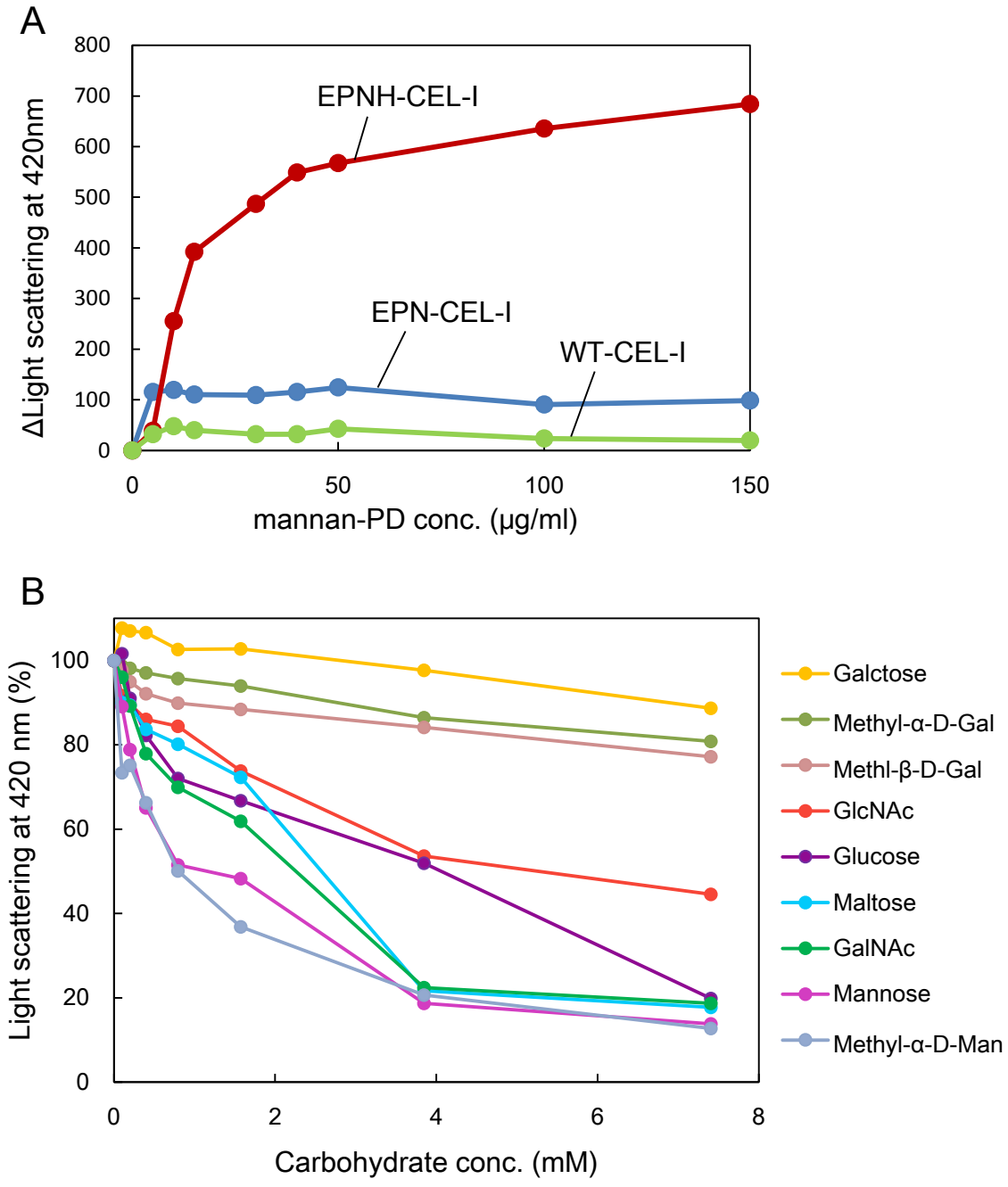
A
800
700
600
500
400
300
200
100
0
ΔLight scattering at 420nm
EPNH-CEL-I
EPN-CEL-I
WT-CEL-I
0
50
100
150
mannan-PD conc. (μg/ml)
B
100
80
60
40
20
0
Light scattering at 420 nm (%)
0
2
4
6
8
Carbohydrate conc. (mM)
Galctose
Methyl-α-D-Gal
Methl-β-D-Gal
GlcNAc
Glucose
Maltose
GalNAc
Mannose
Methyl-α-D-Man

Fig. 4

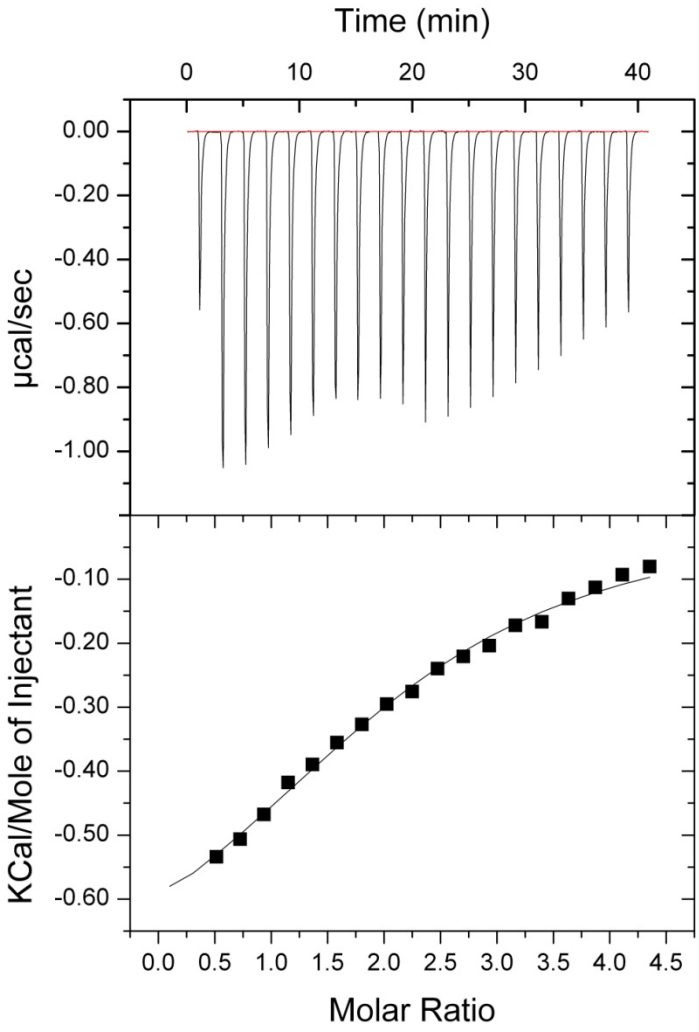
Time (min)
0
10
20
30
40
0.00
-0.20
-0.40
-0.60
-0.80
-1.00
µcal/sec
-0.10
-0.20
-0.30
-0.40
-0.50
-0.60
KCal/Mole of Injectant
0.0
0.5
1.0
1.5
2.0
2.5
3.0
3.5
4.0
4.5
Molar Ratio

Fig. 5

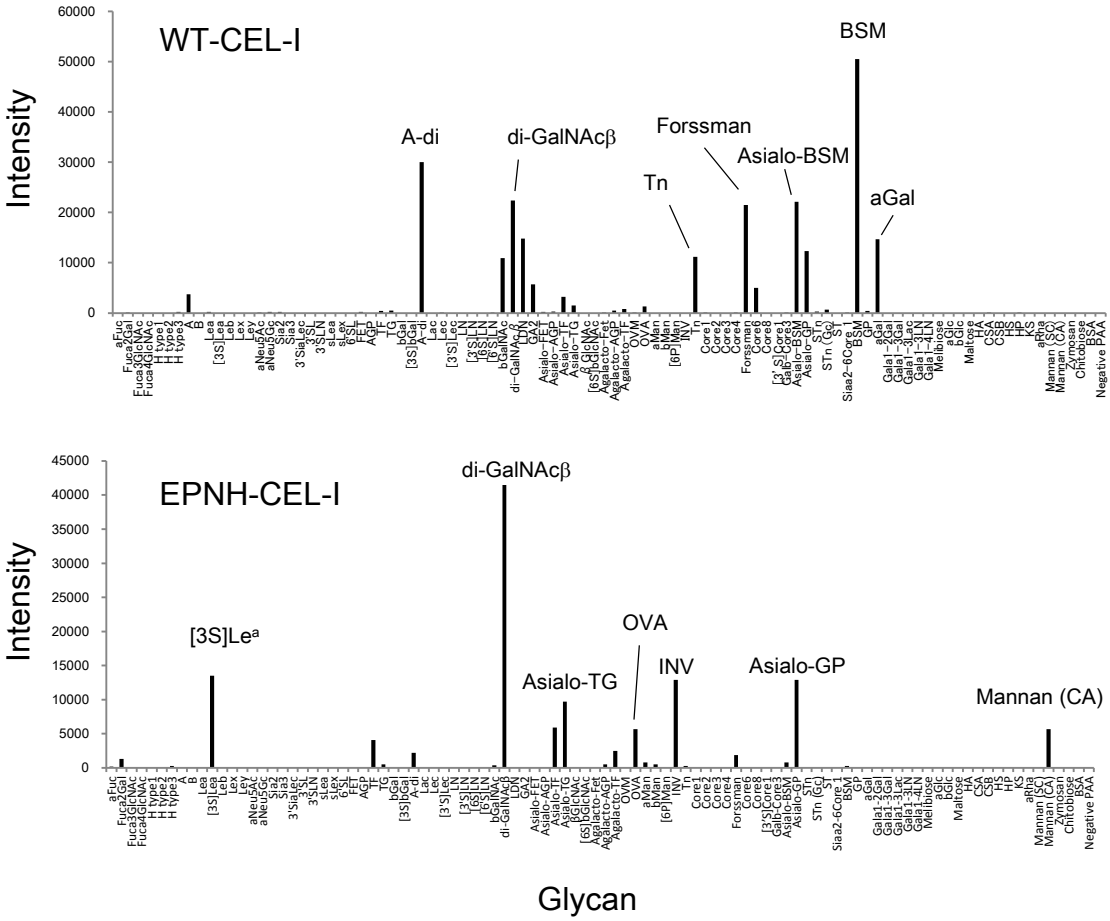
WT-CEL-I
Intensity
A-di
di-GalNAcβ
Tn
Forssman
Asialo-BSM
BSM
aGal
EPNH-CEL-I
Intensity
di-GalNAcβ
[3S]Le^a
OVA
INV
Asialo-TG
Asialo-GP
Mannan (CA)
Glycan

Fig. 6

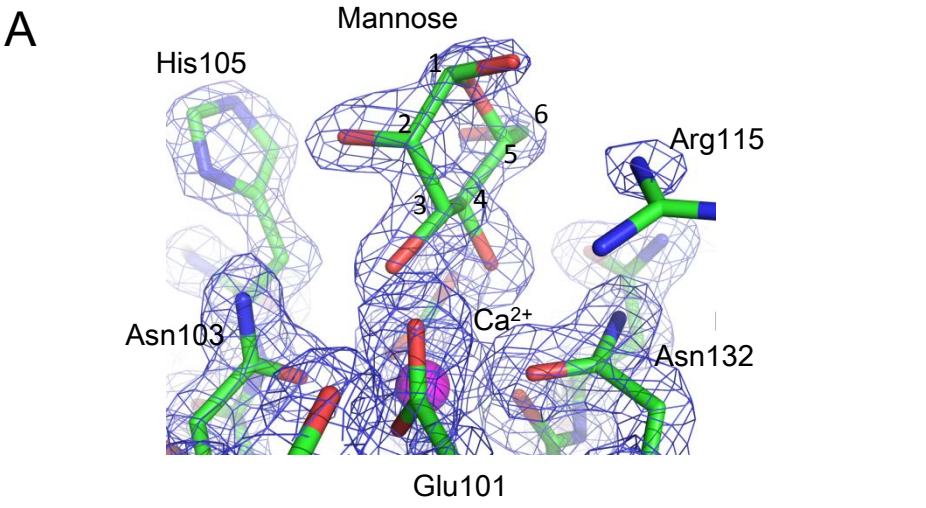

Fig. 7

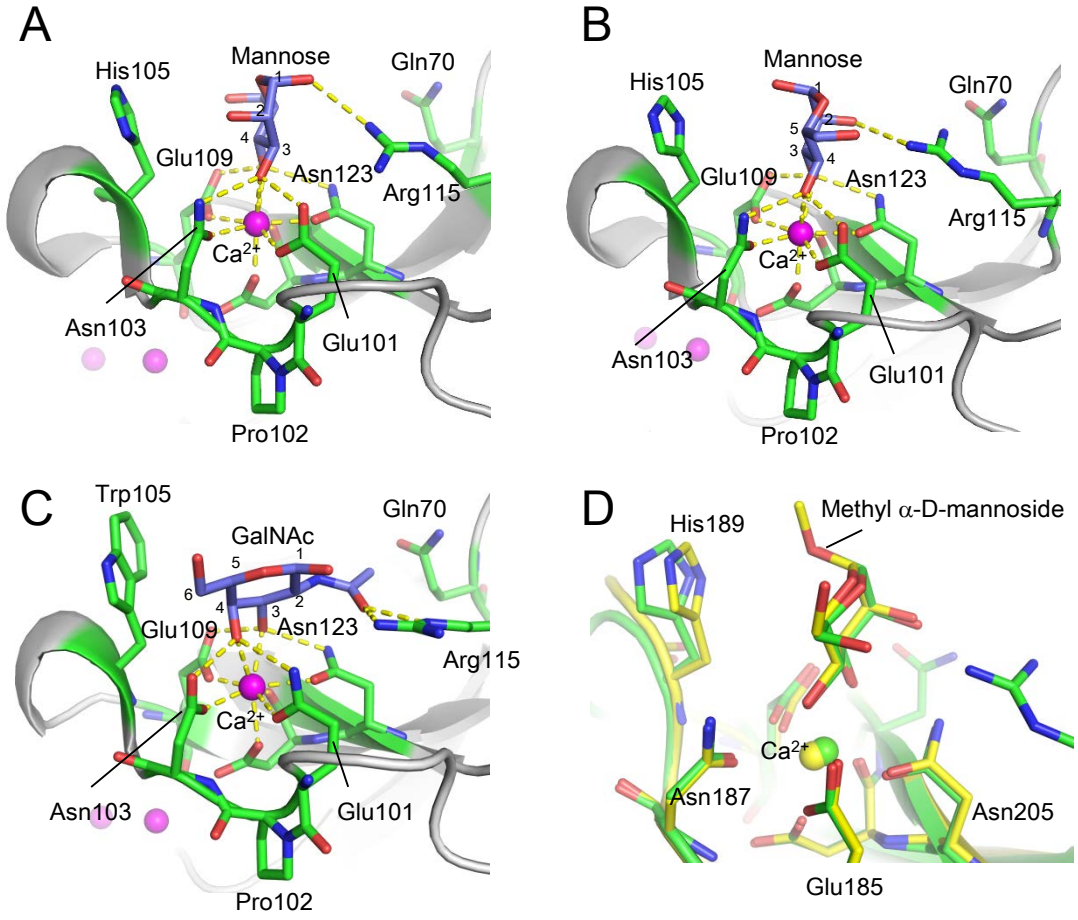
A
His105
Mannose
Gln70
Glu109
Asn123
Arg115
Ca2+
Asn103
Glu101
Pro102
B
His105
Mannose
Gln70
Glu109
Asn123
Arg115
Ca2+
Asn103
Glu101
Pro102
C
Trp105
GalNAc
Gln70
Glu109
Asn123
Arg115
Ca2+
Asn103
Glu101
Pro102
D
His189
Methyl α-D-mannoside
Ca2+
Asn187
Asn205
Glu185

Fig. 8

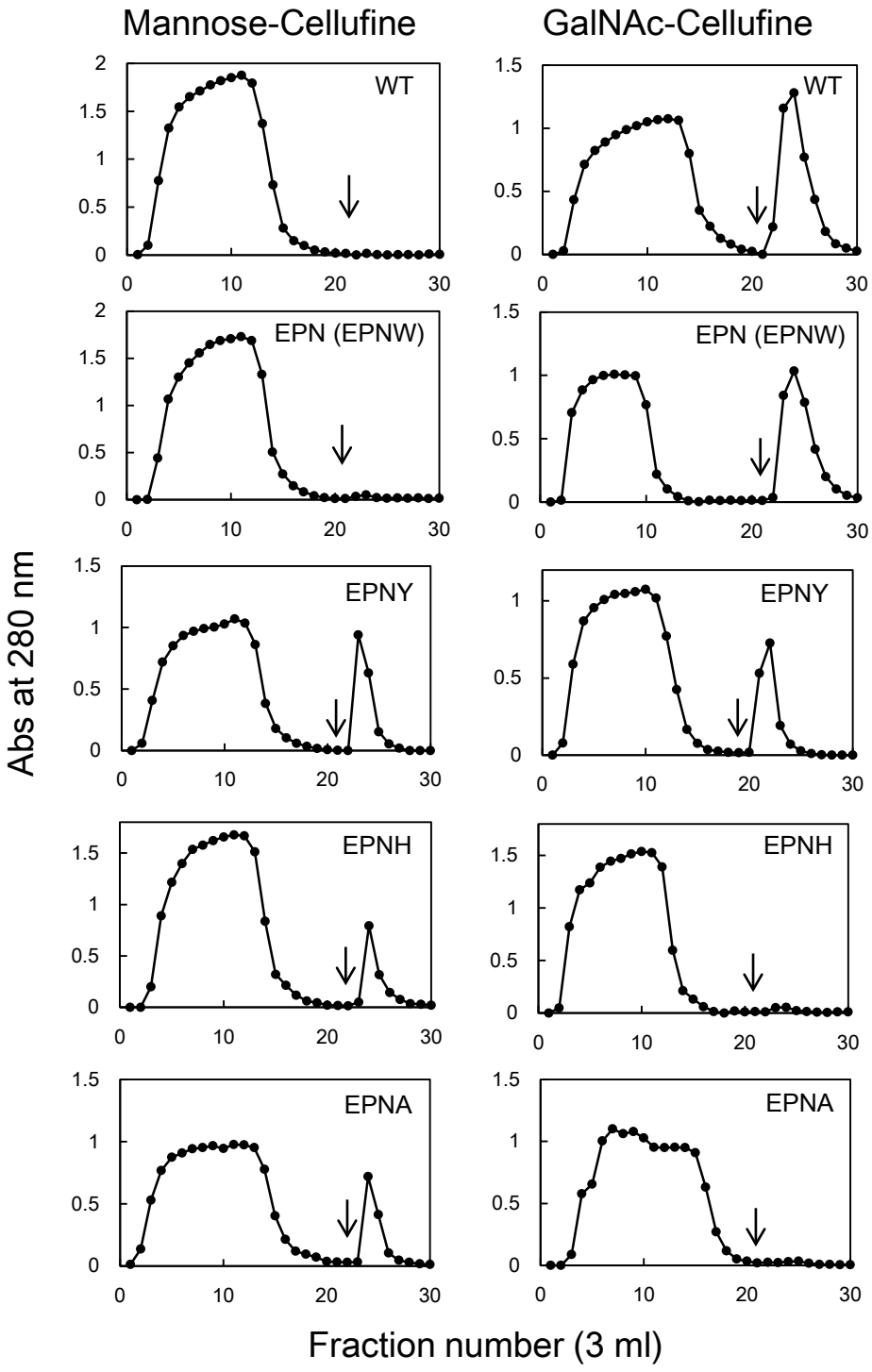
Mannose-Cellufine
GalNAc-Cellufine
WT
WT
EPN (EPNW)
EPN (EPNW)
EPNY
EPNY
EPNH
EPNH
EPNA
EPNA
Abs at 280 nm
Fraction number (3 ml)

Fig. 9